NJC

Accepted Manuscript

This article can be cited before page numbers have been issued, to do this please use: W. Si, X. wang, M. Chen, M. wang, A. Lu and C. Yang, *New J. Chem.*, 2019, DOI: 10.1039/C8NJ05150J.

Journal Name

View Article Online
DOI: 10.1039/C8NJ05150J

ARTICLE

Design, synthesis, antifungal activity and 3D-QSAR study of novel pyrazole carboxamide and niacinamide derivatives containing benzimidazole moiety

Received 00th January 20xx,
Accepted 00th January 20xx

DOI: 10.1039/x0xx00000x

www.rsc.org/

Wei-Jie Si,[abc] Xiao-bin Wang,[ab] Min Chen,[ab] Meng-Qi Wang,[a] Ai-Min Lu[a] and Chun-Long Yang*[abc]

A series of novel pyrazole carboxamide and niacinamide derivatives containing a benzimidazole moiety were designed and synthesized as the antifungal candidate agents. All the target compounds were characterized by FTIR, ^{1}H NMR, ^{13}C NMR , HRMS spectra and elemental analysis. The structure of compound **T1** was further confirmed by single crystal X-ray diffraction analysis. The antifungal activities of the target compounds were evaluated *in vitro* against four phytopathogenic fungi (namely *Botrytis cinerea*, *Rhizoctonia solani*, *Fusarium graminearum* and *Alternaria solani*) by the mycelium growth inhibition method. The bioassay results indicated that some of the compounds exhibited good antifungal activity against *B. cinerea* at 100 ug/mL compared to other three fungi. In order to better explore the structure-activity relationship (SAR), the EC_{50} values of target compounds against *B. cinerea* were further tested and assessed. Subsequently, a 3D quantitative structure–activity relationship (3D-QSAR) study was carried out using the comparative molecular field analysis (CoMFA) technique based on the inhibitory activities against *B. cinerea*. The analysis results from the molecular model revealed fine predictive ability with cross-validated q^2 and non-cross-validated r^2 values of 0.578 and 0.850, respectively.

Introduction

Plant diseases caused by fungi are increasingly recognized as a worldwide threat to crop safety and food security, and has been exacerbated by the increasing frequency of agricultural activities and global trade.[1,2] The use of synthetic pesticides has restrained the occurrence and development of plant fungal diseases, improved the yield and quality of crops,[3] and reduced agricultural economic losses by fighting against highly destructive plant pathogens, such as *Botrytis cinerea,*[4] *Rhizoctonia solani*,[5] *Fusarium graminearum*,[6] and *Alternaria solani.*[7] For example, *Botrytis cinerea*, as an important pathogen of nursery plants, vegetables, ornamental, field, and orchard crops, infects its host plants in all climate areas of the world, infects mainly upper plant parts at pre and post-harvest stages and causes serious damage.[8,9] However, the emergence of drug-resistance, environmental hazards and other problems objectively indicated the urgent need for novel fungicidal candidates.[10,11]

The benzimidazole derivatives have been attracting the attention of organic chemists and pharmacologists for new drug discovery owing to their broad spectrum biological activity and extensive applications,[12] such as, anticancer,[13] anti-inflammatory,[14] antiviral,[15] anti-tubercular,[16] antibacterial,[17] and antifungal activity.[18] In addition, several commercial fungicides containing the benzimidazole scaffold have been applied in the plant disease control, including carbendazim, thiabendazole, and benomyl (Fig. 1). Meanwhile, pyrazole and pyridine, as the biologically active substructures, are usually found in the structures of fungicides. For example, furametpyr (Sumitomo Chemical Co., Ltd., 1997) contains a 5-chloro-1,3-dimethyl-4-pyrazole

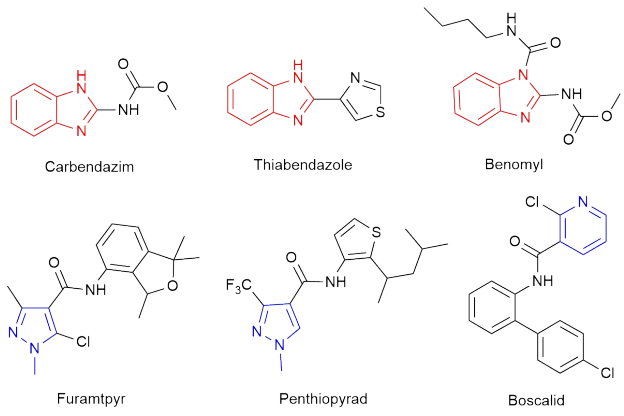

Fig. 1 Commercial fungicides containing benzimidazole, pyrazole or pyridine moiety.

[a] Department of Chemistry, College of Sciences, Nanjing Agricultural University, Nanjing 210095, China.
[b] Jiangsu Key Laboratory of Pesticide Science, Nanjing Agricultural University, Nanjing 210095, China.
[c] Key Laboratory of Monitoring and Management of Crop Diseases and Pest Insects, Ministry of Agriculture, Nanjing Agricultural University, Nanjing 210095, China.
[d] E-mail: ycl@njau.edu.cn. Tel: +86-25-84395207.

†Electronic Supplementary Information (ESI) available: The copies of ^{1}H NMR, ^{13}C NMR, and HRMS spectrograms for all the title compounds can be found in the ESI. See DOI: 10.1039/x0xx00000x

View Article Online
DOI: 10.1039/C8NJ05150J

Journal Name

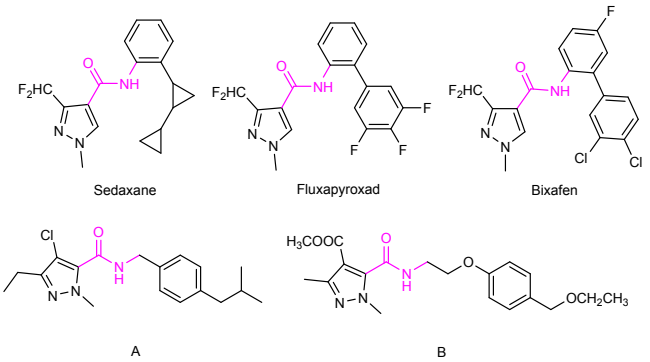

Fig. 2 Representative pyrazole carboxamide compounds with antifungal activities.

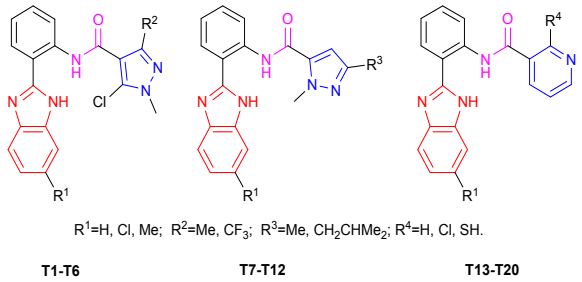

Fig. 3 General structural formulas of target compounds **T1-T20**.

moiety (Fig 1); penthiopyrad (Mitsui Chemicals Co., Ltd., 1996) contains a 1-methyl-3-trifluoromethyl-4-pyrazole moiety (Fig 1); boscalid (BASF, 2003) contains a 2-chloropyridine moiety (Fig. 1), and these substructures are both common pharmacophores in drug development.

The carboxamide fungicides, as a class of well-known fungicides, still play an important role in the agricultural field nowadays, and they have been recently developed with novel structures and superior performance. Sedaxane (Syngenta), fluxapyroxad (BASF), and bixafen (Bayer) were the newly registered fungicides in 2017 and all belonged to the amide compounds (Fig. 2). It is worth noting that most of the commercially available pyrazole amide fungicides are pyrazole-4-carboxamide derivatives. In other words, they possess a carboxamide functional group in 4-position of pyrazole ring. In addition, some studies have shown that pyrazole-5-carboxamide derivatives, such as the compounds A and B, also possessed fungistatic activity (Fig. 2).[19,20]

In the present work, the strategy is to design a novel type of carboxamide compounds with new vitality in antifungal activity via the combination of benzimidazole scaffold with a pyrazole or pyridine moiety through a bridge of formyl aniline group (Fig. 3). In order to better explore the relationship between the effects on the bioactivity caused by structural changes, the pyrazole-4-carboxamide, pyrazole-5-carboxamide and niacinamide derivatives with different substituent groups were synthesized respectively. The antifungal activities of the synthesized compounds were evaluated *in vitro* against four important phytopathogenic fungi, namely *B. cinerea, R. solani*, *F. graminearum* and *A. solani*. The 3D-QSAR based on the inhibitory activities of target compounds against *B. cinerea* was also discussed in detail.

Results and discussion

Chemistry

The synthetic approaches for the two different series of pyrazole-4-carbonyl chlorides **5** and pyrazole-5-carbonyl chlorides **12** are outlined in Scheme 1. The intermediates pyrazole-4-carbonyl chlorides **5a** and **5b** were prepared using an optimized four-step procedure.[21,22] The raw material methylhydrazine was firstly condensed with ethyl acetoacetate **1a** or ethyl 4,4,4-trifluoroacetoacetate **1b** to form 5-hydroxyl-1*H*-pyrazoles **2a** and **2b**, which were treated respectively with $POCl_3$ and DMF (Vilsmeier-Haack chloroformylation) to give pyrazole-4-formaldehydes **3a** and **3b**. The compound **3** was then treated with potassium permanganate to provide pyrazole-4-carboxylic acids **4a** and **4b**. The intermediates **5** were finally obtained by the reaction of the acids **4** with thionyl chloride.

The intermediates pyrazole-5-carbonyl chlorides **12a** and **12b** were prepared using an optimized five-step procedure.[23,24] The raw material diethyl oxalate **6** was firstly reacted with acetone **7a** or 4-methyl-2-pentanone **7b** in the presence of sodium ethoxide to produce ethyl 2,4-dioxovalerate **8a** and ethyl 6-methyl-2,4-dioxoheptanoate **8b**, which were further reacted respectively with hydrazine

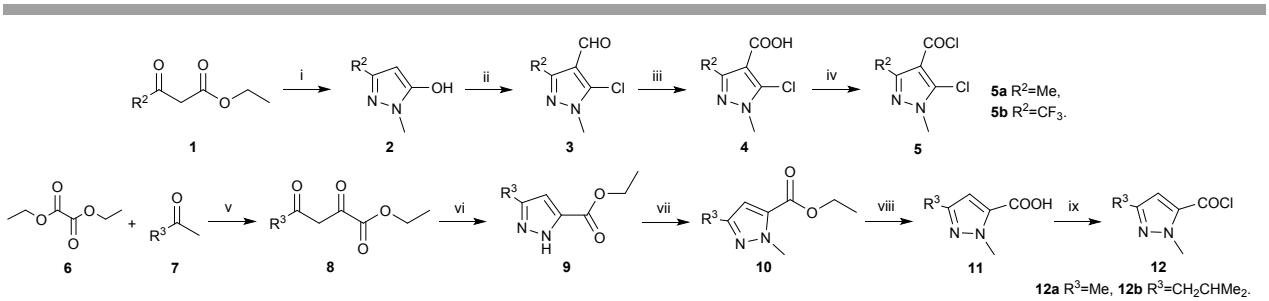

Scheme 1 Synthetic route to pyrazole intermediates **5** and **12**. Reagents and conditions: (i) methyl hydrazine, EtOH, 65 °C for 3 h, then reflux for 5 h; (ii) $POCl_3$, DMF, rt for 1 h, 55 °C for 2 h, then 100 °C for 5 h; (iii) $KMnO_4$, H_2O, 80 °C, 4 h; (iv) $SOCl_2$, reflux, 6 h; (v) EtONa, anhydrous EtOH, -5 °C, 3 h; (vi) hydrazine hydrate, EtOH, 0 °C, 1 h; (vii) Me_2SO_4, DMF, 60 °C, 3 h; (viii) NaOH, THF, H_2O, 70 °C, 2 h, (iX) $SOCl_2$, reflux, 6 h.

View Article Online
DOI: 10.1039/C8NJ05150J

hydrate to give ethyl pyrazole-5-carboxylates **9**. Dimethyl sulfate was used for the methylation reaction with **9** to give ethyl 1-methyl-1*H*-pyrazole-5-carboxylates **10**, which were then hydrolyzed to give the pyrazole-5-carboxylic acids **11**. The intermediates **12** were finally obtained by the reaction of the acids **11** with thionyl chloride.

In above two synthetic routes, different raw materials and reaction conditions were used to synthesize the pyrazole intermediates pyrazole-4-carbonyl chlorides and pyrazole-5-carbonyl chlorides. The most key steps were the cyclization reactions of different pyrazole rings. When methylhydrazine was used for the cyclization of compound **2**, it was necessary to maintain the relatively high temperature (reflux) and long reaction time (5 h). When hydrazine hydrate was used for the cyclization of compound **9**, it is necessary to maintain the relatively low temperature (−5 °C) and short reaction time (3 h).

Another kind of key intermediates 2-(benzimidazol-2-yl)phenylamines **16** were obtained by using an optimized three-step procedure.[25,26] As displayed in Scheme 2, the raw material 2-nitrobenzaldehyde **13** was firstly reacted with sodium bisulfite to prepare sodium hydroxy(2-nitrophenyl)methanesulfonate **14**. This salt was reacted respectively with three substituted *o*-phenylenediamines to give the cyclized products **15**. After the reduction reaction using stannous chloride, the intermediates **16** were obtained in the yields of 40% above.

The target compounds **T1**–**T20** were finally synthesized by the amidation reaction. The synthetic route was shown in Scheme 3. Two amidation methods were used to synthesize the target compounds. When the pyrazole carboxamide derivatives **T1**–**T12** were synthesized, the pyrazole carbonyl chlorides **5** and **12** were reacted respectively with the benzimidazole intermediates in the presence of Et_3N. When the niacinamide derivatives **T13**–**T20** were synthesized, the substituted nicotinic acids were directly used to react with different benzimidazole intermediates in the presence of TBTU (*O*-(benzotriazol-1-yl)-*N*,*N*,*N*',*N*'-tetramethyluronium tetrafluoroborate) and Et_3N.

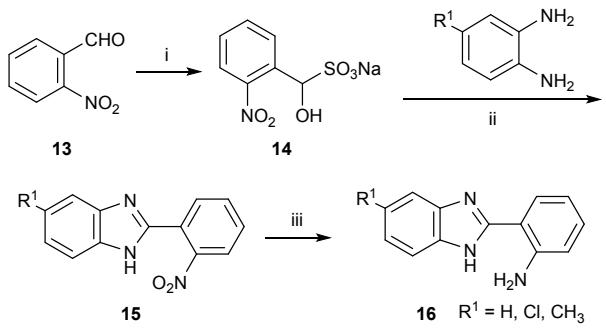

Scheme 2 Synthetic route to benzimidazole intermediates **16**. Reagents and conditions: (i) $NaHSO_3$, EtOH, H_2O, rt, 15 min; (ii) DMF, reflux, 3 h; (iii) $SnCl_2{\cdot}2H_2O$, EtOH, reflux, 0.5-1 h.

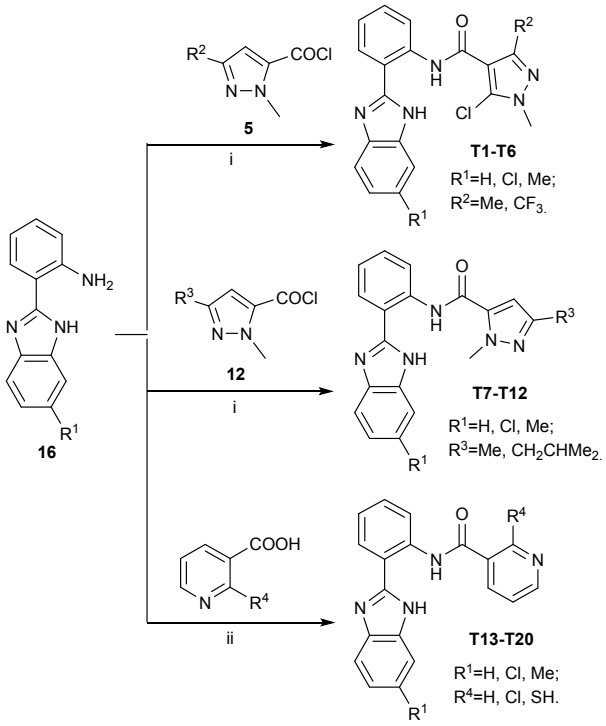

Scheme 3 Synthetic route to target compounds **T1-T20**. Reagents and conditions: (i) Et_3N, CH_2Cl_2, rt, overnight; (ii) TBTU, Et_3N, CH_2Cl_2, rt, overnight.

Crystal structure of compound T1

The structure of compound **T1** was further studied using the single crystal X-ray analysis. The corresponding crystal structure was shown by Fig. 4. The crystal data for **T1**: monoclinic, a = 9.2973(4) Å, b = 16.7097(7) Å, c = 11.0503(5) Å, α = 90 °, β = 94.760(4) °, γ = 90 °, V = 1710.80(13) Å^3, Z = 4, space group P21/c (no.14), μ = 0.242 mm^{-1}, D_{calc} =1.420 g/cm^3, 7766 reflections measured (4.4≤2ϑ≤52.8), 4000 unique (R_{int} = 0.048) were used in all calculations. The final R_1 was 0.0428 (I>2σ(I)) and $wR(F_2)$ was 0.1021. The crystallographic data have been deposited with the Cambridge Crystallographic Data Centre. The deposition number was CCDC1865306.

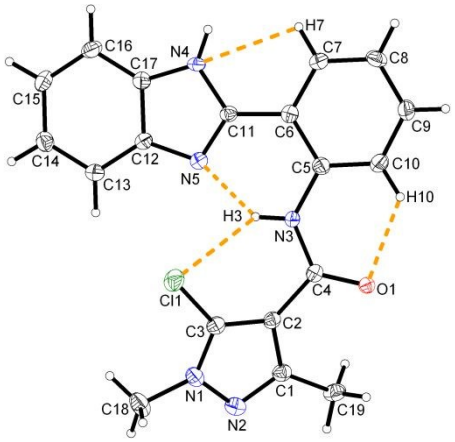

Fig 4. Crystal structure diagram of compound **T1**.

Antifungal activity

The antifungal activities of target compounds **T1**–**T20** against four fungi were assayed with hymexazol as the positive control at 100 ug/mL. As can be seen from table 1 that the target

compounds showed better inhibitory activity against *B. cinerea*

View Article Online
DOI: 10.1039/C8NJ05150J

Table 1 Inhibitory rates of target compounds **T1**-**T20** against four phytopathogenic fungi at 100 ug/mL

Compound	R^1	R^2	R^3	R^4	*B. cinerea*	*R. solani*	*F. graminearum*	*A. solani*
T1	H	Me	–	–	65.53±0.40	64.34±0.31	39.21±0.34	29.71±0.37
T2	H	CF_3	–	–	83.11±0.21	64.84±0.22	52.37±0.17	34.57±0.31
T3	Cl	Me	–	–	72.37±1.30	62.34±0.17	51.58±0.42	52.57±0.21
T4	Cl	CF_3	–	–	79.68±0.31	69.08±0.33	52.63±0.05	58.28±0.49
T5	Me	Me	–	–	85.62±0.34	64.34±0.54	45.52±0.34	66.00±0.17
T6	Me	CF_3	–	–	85.39±0.21	62.84±0.31	47.37±0.21	68.28±0.67
T7	H	–	Me	–	43.38±0.42	38.65±0.86	21.05±0.00	21.42±0.40
T8	H	–	CH_2CHMe_2	–	45.66±0.49	30.17±1.41	18.42±0.21	29.14±1.38
T9	Cl	–	Me	–	44.98±0.17	39.90±0.65	22.36±0.17	24.57±0.08
T10	Cl	–	CH_2CHMe_2	–	52.28±1.08	36.66±0.21	25.79±0.06	34.00±0.22
T11	Me	–	Me	–	52.28±1.08	34.91±1.09	17.36±0.42	62.57±0.31
T12	Me	–	CH_2CHMe_2	–	41.55±0.61	45.38±0.50	25.00±0.22	30.85±0.21
T13	H	–	–	H	52.05±1.29	40.15±0.02	21.05±0.04	22.85±0.07
T14	H	–	–	Cl	88.13±0.56	69.82±0.17	41.58±0.26	40.00±0.21
T15	H	–	–	SH	44.75±0.42	28.67±0.88	19.47±0.37	30.28±0.21
T16	Cl	–	–	H	32.42±0.61	33.91±1.87	15.52±0.22	24.57±0.03
T17	Cl	–	–	Cl	55.02±2.93	44.89±0.98	24.21±0.37	34.28±0.21
T18	Cl	–	–	SH	35.39±0.70	22.69±0.67	29.21±0.17	25.14±0.21
T19	Me	–	–	H	31.74±0.91	26.43±0.60	14.73±0.06	28.00±0.63
T20	Me	–	–	Cl	74.66±0.50	67.33±0.48	43.15±0.07	58.85±0.04
Hymexazol	–	–	–	–	100.00	72.82±0.17	68.16±0.17	55.43±0.37

than the other three fungi. Most of the compounds presented moderate to good antifungal activity against *B. cinerea in vitro*. In particular, among the compounds tested, **T2**, **T5**, **T6** and **T14** exhibited excellent activities with the inhibition rates as high as 83.11%, 85.62%, 85.39% and 88.13%. Additionally, some compounds also exhibited obvious inhibitory activity against *R. solani* and *A. solani*. The inhibition rates of compounds **T1**–**T6**, **T14**, and **T20** exceeded 60% against *R. solani*. And the inhibition rates of compounds **T4**–**T6**, **T11** and **T20** ranged from 58.28% to 68.28% against *A. solani*, which were better than 55.43% of the control hymexazol.

Based on the results of the preliminary screening, the EC_{50} values of the title compounds against *B. cinerea* were evaluated and summarized in Table 2. The compounds **T5** and **T6** exhibited encouraging antifungal activities against *B. cinerea* with EC_{50} values of 18.24 and 10.16 ug/mL, respectively. When substituted pyrazoles were introduced, the target compounds with pyrazole-4-carboxamide moiety showed higher activities than the target compounds with pyrazole-5-carboxamide moiety. For example, the activities of **T1** and **T2** were better than those of **T7** and **T8**, the activities of **T3** and **T4** were better than those of **T9** and **T10**, and the activities of **T5** and **T6** were better than those of **T11** and **T12**. In the target compounds containing pyrazole-4-carboxamide moiety, the compounds with CF_3 group at R^2 position were more active than the compounds with CH_3 group at R^2 position. That is to say, the compounds **T2**, **T4** and **T6** showed better activity than **T1**, **T3** and **T5**, respectively. When substituted pyridines were introduced, the activities of targets with 2-chlorine-niacinamide were superior than other niacinamide products. For example, the activity of compound **T14** was superior to that of **T13** and **T15**, the activity of compound **T17** was superior to that of **T16** and **T18**, and the

Table 2 EC_{50} values of target compounds **T1**-**T20** against *B. cinerea*

Compound	Regression equation	EC_{50} (ug/ml)	r
T1	y = 1.5740x+2.2330	57.27±0.40	0.9812
T2	y = 1.8298x+2.1726	35.09±0.32	0.9878
T3	y = 1.2895x+2.9740	37.25±0.29	0.9795
T4	y = 1.5838x+2.5535	35.04±0.34	0.9821
T5	y = 1.3517x+3.2953	18.24±0.36	0.9716
T6	y = 0.9867x+4.0063	10.16±0.26	0.9726
T7	y = 1.5565x+1.9229	94.82±0.42	0.9787
T8	y = 1.7151x+1.4811	112.63±0.29	0.9914
T9	y = 0.9127x+2.9113	194.25±0.18	0.9881
T10	y = 1.0533x+2.5913	193.61±0.16	0.9930
T11	y = 1.6850x+1.5565	110.57±0.48	0.9761
T12	y = 1.4714x+2.0347	103.57±0.14	0.9972
T13	y = 1.6975x+1.7669	80.28±0.39	0.9847
T14	y = 1.6931x+2.5975	26.24±0.37	0.9808
T15	y = 1.6027x+1.5433	143.48±0.27	0.9912
T16	y = 1.3403x+2.2538	111.92±0.38	0.9760
T17	y = 1.2197x+2.5777	96.81±0.33	0.9779
T18	y = 1.6049x+1.6830	116.64±0.42	0.9802
T19	y = 1.1698x+2.4282	157.92±0.34	0.9754
T20	y = 1.4928x+2.6659	36.60±0.24	0.9897
Hymexazol	y = 0.6466x+4.2544	14.22±0.05	0.9920

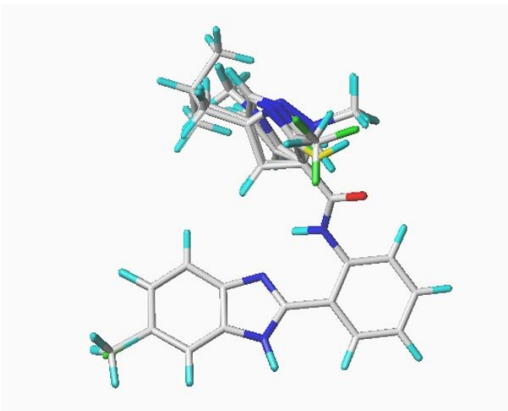

Fig. 5 Alignment of all title compounds to common template molecule **T6**.

View Article Online
DOI: 10.1039/C8NJ05150J

Table 3 Experimental and predicted pEC_{50} results against *B. cinerea*

Compound	Experimental[a]	Predicted[b]	Residual[c]
T1	3.804	3.996	-0.192
T2*	4.077	4.306	-0.229
T3	4.030	3.950	0.080
T4	4.112	4.257	-0.146
T5	4.318	4.198	0.120
T6	4.629	4.512	0.118
T7	3.543	3.435	0.108
T8	3.520	3.433	0.088
T9*	3.274	3.392	-0.118
T10	3.323	3.386	-0.063
T11	3.494	3.624	-0.130
T12*	3.573	3.626	-0.054
T13	3.592	3.434	0.159
T14*	4.123	3.610	0.513
T15	3.382	3.544	-0.161
T16	3.493	3.389	0.104
T17	3.596	3.565	0.031
T18	3.513	3.501	0.012
T19	3.318	3.633	-0.314
T20	3.995	3.809	0.187

[a] Experimental pEC_{50};
[b] Predicted pEC50 by CoMFA;
[c] Relative error of experimentally predicted pEC_{50};
* Samples of test set.

Table 4 Statistical parameters for CoMFA model

Statistical parameter	CoMFA	Validation criteria
q^2 [a]	0.578	> 0.5
ONC [b]	3	
r^2 [c]	0.850	> 0.8
SEE[d]	0.166	
F [e]	22.661	
Fraction of field contributions [f]		
Steric	0.516	
Electrostatic	0.484	

[a] Cross-validated correlation;
[b] Optimum number of components;
[c] Noncross-validated correlation;
[d] Standard error of estimate;
[e] F-test value;
[f] Field contributions: steric and electrostatic.

compounds were superior to the H and SH-substituted compounds. In other words, the compounds fell into order by activity as **T14**>**T13**>**T15**, and **T17**>**T16**>**T18**.

Performance of CoMFA model

A total of sixteen title compounds were randomly chosen as the training set, and the remaining four compounds (labeled with asterisks) were used as the test set. The 3D structures of twenty title molecules were aligned to the common template molecule of **T6** with the best antifungal activity against *B. cinerea* and are showed on Fig. 5. Based on the experimental pEC_{50} values of the training set in Table 3, the CoMFA model was developed for the 3D-QSAR study, and their calculated statistical parameters are shown in Table 4. The results in Table 4 indicated that the cross-validated coefficient q^2, non-cross-validated correlation coefficient r^2, SEE and F of the activity of **T20** was superior to that of **T19**. Furthermore, the Cl-substituted model were 0.578 with 3 ONC, 0.850, 0.166, and 22.661, respectively. The values of q^2 and r^2 in the CoMFA model were better than the standard reference values of 0.5 (q^2) and 0.8 (r^2), which manifested the good predictive ability of the obtained 3D-QSAR model.[27,28] Meanwhile, as shown in Table 4, the contributions of steric field and electrostatic field to the CoMFA model were 0.516 and 0.484 respectively, which suggested that the bioactivity was mainly determined by the steric interactions. Using the obtained CoMFA model as a test tool, the predicted pEC_{50} values of title compounds agsinst *B. cinerea* in the training and test sets were predicted and presented in Table 3. As presented in Fig. 6, the correlation between the predicted and experimental pEC_{50} values in the CoMFA model also demonstrated the good predictive ability of the obtained CoMFA model.

CoMFA contour map analysis

In the CoMFA contour maps of the steric (Fig. 7A) and electrostatic (Fig. 7B) fields, the title compound **T6**, which possesses the best antifungal activity against *B. cinerea*, are shown inside to better understand the structural features of synthesized compounds. As shown in Fig. 7A, there are two larger yellow contours closely around the pyrazole scaffold, which indicates that the bulky substituted groups at these regions are unfavorable for their biological activity. This can explain that the compounds **T8, T10** and **T12** bearing an

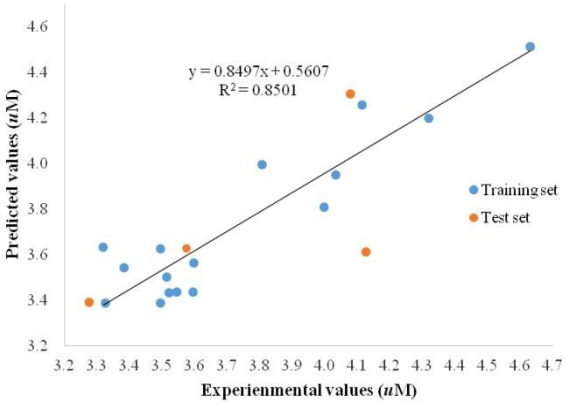

Fig. 6 Correlation between predicted and experimental pEC_{50} values in CoMFA model.

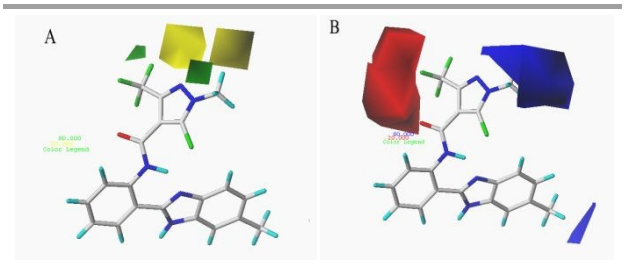

Fig. 7 CoMFA contour maps of steric and electrostatic fields. (A) Sterically favored areas for bioactivity are in green, and sterically disfavored areas for bioactivity are in yellow; (B) Electron-withdrawing favored areas for bioactivity are in red, and electron-withdrawing disfavored areas for bioactivity are in blue.

isobutyl at the 3-position of pyrazole-5-yl scaffold had notgood fungicidal activity. Meanwhile, the Fig. 7A shows two green contours around the 1-and 3-positions of pyrazole scaffold, which suggests that introducing suitable bulky substitutes into these regions are favorable for their antifungal activity. It was confirmed that the compounds **T1**–**T6** bearing a methyl at 1-position and a methyl or trifluoromethyl at 3-position of pyrazole-4-yl scaffold exhibited higher antifungal activity.

As shown in Fig. 7B, a large blue contour near the 1-position of pyrazole scaffold indicates that electron-donating substitutes at this region are helpful for the increase of antifungal activity, such as the compounds **T1**–**T6**. A large red contour between the carbonyl group and the 3-position of pyrazole ring indicates the carboxamide group played a pivotal role in maintaining their antifungal activity. Meanwhile, the large red contour also demonstrates that introducing a electron-withdrawing group at the 3-position of pyridine ring would increase their bioactivity. For example, the compounds **T14** and **T20** containing chlorine atoms at the R^4 position of pyridine ring showed good antifungal activity against *B. cinerea*. In addition, a small blue contour near the 6-position of benzimidazole scaffold indicates that the electron-donating substitutes are favorable for their biological activity, which agrees with the fact that the title compounds **T5** and **T6** contributed the highest antifungal activity.

Conclusion

In summary, the pyrazole carboxamide and niacinamide derivatives containing a benzimidazole moiety were prepared and evaluated for their antifungal activities against four pathogenic fungi. The structures of these compounds were well identified by spectral data and single crystal X-ray diffraction. The bioassay results showed that some of the compounds possessed good antifungal activity against *B. cinerea in vitro*. In particular, the compounds **T5** and **T6** exhibited high antifungal activities with EC_{50} values of 18.24 and 10.16 ug/mL, respectively. The established CoMFA model based on the anti-*B. cinerea* activities of the target compounds showed fine predictive ability. The present work demonstrated that pyrazole carboxamide and niacinamide derivatives containing a benzimidazole moiety can effectively control the fungus *B. cinerea*. Further structural optimization of the target compounds and other related experiments are ongoing in our laboratory.

Experimental

The melting points of the products were determined using a SMP50 Automatic Melting Point Apparatus and were not corrected. The ^{1}H NMR and ^{13}C NMR spectra were captured with a Bruker Avance III 400 NMR spectrometer at room temperature with TMS as the internal standard. The Tin-layer chromatography (TLC) was performed on silica gel GF254. The high resolution mass spectrometer was recorded on an Agilent Technologies 6540 UHD Accurate-Mass Q-TOF LC/MS using ESI. All the reagents were of pure analytical grade and used directly without further treatment unless otherwise noted.

Synthesis of pyrazole-4-carbonyl chlorides 5

The solution of 40% methylhydrazine (0.06 mol) was heated to 65 °C, and the raw material ethyl acetoacetate **1a** or ethyl 4,4,4-trifluoroacetoacetate **1b** (0.05 mol) was added dropwise. The reaction mixture was maintained at 65 °C for 3 h, and then it was heated to reflux for another 5 h. The solvent was evaporated under reduced pressure to afford the yellow solids 1,3-dimethyl-5-hydroxyl-1*H*-pyrazole **2a** (75.4%) and 1-methyl-3-trifluoromethyl-5-hydroxyl-1*H*-pyrazole **2b** (80.3%).

To a violently stirred cold solution (−5°C) of DMF (0.1 mol) was added dropwise phosphorus oxychloride (0.15 mol). The resulting mixture was stirred at room temperature for 1 h. To the above mixture was added the compound **2** (0.05 mol) in portions, it was then heated to 55 °C for 2 h and stirred at 100 °C for another 5 h. After cooling to room temperature, the mixture was poured into ice-water (200 mL), and the resulting precipitate was collected by filtration. The filtrate was continuously extracted with ethyl acetate (3 × 50 mL), and the organic layer was dried over anhydrous magnesium sulfate. The solvent was removed under reduced pressure to give a brown solid. The solid obtained above in two portions was collected together as the products 5-chloro-1,3-dimethyl-1*H*-pyrazole-4-formaldehyde **3a** (76.3%) and 5-chloro-1-methyl-3-trifluoromethyl-1*H*-pyrazole-4-formaldehyde **3b** (79.6%).

The compound **3** (0.025 mol), acetone (5 mL), and water (25 mL) were added in a 250 mL three-neck round-bottom flask. The solution was stirred and slowly warmed up to 60 °C. Then, a solution of potassium permanganate (0.0275 mol) and water (50 mL) was added dropwise, and heated to 80 °C for 4 h. The solution was cooled and filtered, concentrated hydrochloric acid was slowly added until the pH<2. A large amount of white solid was precipitated, filtered, washed with water, and dried to give the white solids 5-chloro-1,3-dimethyl-1H-pyrazole-4-carboxylic acid **4a** (70.2%) and 5-chloro-1-methyl-3-trifluoromethyl-1H-pyrazole-4-carboxylic acid **4b** (76.1%).

The pyrazole-4-carboxylic acids **4** were reacted respectively with thionyl chloride under reflux for 6 h. The excessive thionyl chloride was removed under reduced pressure to obtain 5-chloro-1,3-dimethyl-1*H*-pyrazole-4-carbonyl chloride **5a** and 5-chloro-1-methyl-3-trifluoromethyl-1*H*-pyrazole-4-carbonyl chloride **5b**.

Synthesis of pyrazole-5-carbonyl chlorides 12

The mixed solution of diethyl oxalate **6** (0.105mol) and acetone **7a** (or 4-methyl-2-pentanone **7b**) (0.1 mol) was added slowly to the cooled (−10°C) solution of sodium ethoxide (0.128mol) and ethonal (100 mL). The obtained mixture was stirred at −5°C for 3 h and then poured into ice water, adjusted pH to 4 with 10% dilute hydrochloric acid, and extracted with ethyl acetate. The organic layer was washed twice with water and dried over anhydrous Na_2SO_4, filtered and concentrated under reduced pressure to give the yellow liquids ethyl 2,4-

dioxovalerate **8a** (85.8%) and ethyl 6-methyl-2,4-dioxoheptanoate **8b** (80.4%).

The compound **8** (0.05 mol) was dissolved in ethanol (50 mL) and cooled to −10°C. 80% Hydrated hydrazine (0.0625 mol) was added dropwise to the above solution, and kept stirring below 0°C for 1 h. The solvent was evaporated under reduced pressure. Water (100 mL) was added to the residue, and the mixture was extracted with ethyl acetate (3 × 20 mL). The organic layer was washed twice with water, dried over anhydrous Na_2SO_4, filtered, and concentrated under pressure to give the pale yellow solids ethyl 3-methyl-1*H*-pyrazole-5-carboxylate **9a** (88.4%) and ethyl 3-isobutyl-1*H*-pyrazole-5-carboxylate **9b** (73.8%).

The compound **9** (0.04mol) and dimethyl sulfate (0.048 mol) were dissolved in DMF, and the solution was stirred at 60°C for 3 h. The progress of reaction was monitored by TLC. After complete disappearance of the starting material, the reaction solution was poured into water (100 mL) and extracted with ethyl acetate (3 × 25 mL). The organic phase was washed twice with water, dried over anhydrous $MgSO_4$, filtered, and concentrated under reduced pressure to give ethyl 1,3-dimethyl-1*H*-pyrazole-5-carboxylate **10a** (85.1%) and ethyl 1-methyl-3-isobutyl-1*H*-pyrazole-5-carboxylate **10b** (77.3%).

20% Sodium hydroxide solution (0.12 mmol) was added to a solution of compound **10** (0.1 mmol) in THF, stirred at 70 °C for 2 h. The solution was concentrated in vacuo to remove most of the THF. The pH was adjusted to 3–4 with 10% dilute hydrochloric acid. The mixture was filtered, and the filter cake was washed with water to give 1,3-dimethyl-1*H*-pyrazole-5-carboxylic acid **11a** (68.4%) and 1-methyl-3-isobutyl-1*H*-pyrazole-5-carboxylic acid **11b** (65.9%). Finally, the same synthesis method as the intermediates **5** was used to prepare 1,3-dimethyl-1*H*-pyrazole-5-carbonyl chloride **12a** and 1-methyl-3-isobutyl-1*H*-pyrazole-5-carbonyl chloride **12b**.

Synthesis of 2-(benzimidazol-2-yl)phenylamines 16

2-Nitrobenzaldehyde **13** (0.05 mol) and sodium bisulfite (0.05 mol) were dissolved in ethanol (30 mL) and water (30 mL), respectively, and then mixed and stirred for 15 min at room temperature. The reaction mixture was filtered to obtain sodium hydroxy(2-nitrophenyl)methanesulfonate **14**. The resulting salt (0.02 mol) and *o*-phenylenediamine (0.02 mol) in DMF (60 mL) were refluxed for 3 h in an oil bath. After the reaction mixture was poured onto crushed ice, 2-(2-nitrophenyl)-1*H*-benzimidazole **15** was separated by filtration and recrystallized from a methanol/water mixture (V/V = 1:1). The mixture of compound **15** (0.05 mol) and $SnCl_2{\cdot}2H_2O$ (0.25 mol) in ethanol (50 mL) was refluxed for 0.5–1 h. The reaction mixture was cooled to room temperature. And 10% NaOH solution was then added in small portions in an ice-water bath until the mixture became strongly alkaline (pH>11). The resulting mixture was extracted with ethyl acetate (4 × 100 mL). The combined extracts were washed with brine, dried over anhydrous Na_2SO_4, filtered and evaporated in vacuo to give 2-(1*H*-benzimidazol-2-yl)phenylamine **16a** (45.4%), 2-(6-chloro-1*H*-benzimidazol-2-yl)phenylamine **16b** (48.7%), and 2-(6-methyl-1*H*-benzimidazol-2-yl)phenylamine **16c** (40.2%).

Synthesis of target compounds T1–T20

The pyrazole carbonyl chloride **5** or **12** (3 mmol) in dichloromethane (25 mL) was slowly added to a solution of corresponding benzimidazole-2-phenylamine **16** (3 mmol) and triethylamine (6 mmol) in dichloromethane at a controlled temperature of 0–5 °C. The reaction mixture was stirred at room temperature overnight and then was washed with water, dried, and evaporated under reduced pressure to obtain a solid. The solid was purified by column chromatography to give a desired product the pyrazole carboxamide derivative containing a benzimidazole moiety. The yields of obtained target compounds **T1**–**T12** ranged from 41.3% to 70.6%.

The nicotinic acid (3 mmol) and TBTU (3.6 mmol) were added to dichloromethane (30mL). Triethylamine (6 mmol) was then added dropwise, and the mixture was stirred for 30 min. After the corresponding benzimidazolee-2-phenylamine **16** (3 mmol) was added to the mixture, stirring was continued overnight at room temperature. The reaction mixture was then filtered. The resulting solid was washed with water and dried to give a target product the niacinamide derivative containing a benzimidazole moiety. The yields of obtained target compounds **T13**–**T20** ranged from 42.0% to 80.5%.

N-(2-(1H-Benzimidazol-2-yl)phenyl)-5-chloro-1,3-dimethyl-1H-pyrazole-4-carboxamide (T1): White solid, yield 70.6%, mp 240-242 °C; IR (KBr) (ν_{max}/cm^{-1}): 3288, 2863, 1646, 1625, 1587, 1542, 1429, 1366, 1328, 1146, 968, 902, 554. ^{1}H NMR (400 MHz, DMSO-d_6) δ: 13.32 (s, 1H), 13.22 (s, 1H), 8.78 (d, J = 8.4 Hz, 1H), 8.25–8.11 (m, 1H), 7.64 (dd, J = 15.7, 7.2 Hz, 2H), 7.54 (t, J = 7.8 Hz, 1H), 7.32 (t, J = 7.6 Hz, 3H), 3.87 (s, 3H), 2.48 (s, 3H). ^{13}C NMR (101 MHz, DMSO-d_6) δ: 160.6, 151.0, 148.2, 142.4, 138.6, 134.0, 131.0, 127.8, 127.5, 123.8, 123.5, 122.7, 121.2, 118.8, 116.3, 113.6, 111.9, 36.6, 14.2. HRMS (ESI) Calcd for $C_{19}H_{17}ClN_5O$ [M+H]$^+$: 366.11161, found: 366.11169. Anal. Calcd for C, 62.38; H, 4.41; N, 19.14. Found: C, 62.65; H, 4.80; N, 18.80%.

***N*-(2-(1*H*-Benzimidazol-2-yl)phenyl)-5-chloro-1-methyl-3-(trifluoromethyl)-1*H*-pyrazole-4-carboxamide (T2)**: Pale yellow solid, yield 58.4%, mp 254-256 °C; IR (KBr) (ν_{max}/cm^{-1}): 3247, 2934, 1661, 1610, 1587, 1533, 1485, 1450, 1432, 1372, 1325,1274, 1188, 1149, 1024, 959, 905, 751. ^{1}H NMR (400 MHz, DMSO-d_6) δ: 13.92 (s, 1H), 13.30 (s, 1H), 8.80 (d, J = 8.3 Hz, 1H), 8.30–8.14 (m, 1H), 7.66 (s, 2H), 7.61–7.53 (m, 1H), 7.42–7.34 (m, 1H), 7.30 (s, 2H), 4.07 (s, 3H). ^{13}C NMR (101 MHz, DMSO-d_6) δ: 157.9, 150.8, 139.2 (q, J= 38.3 Hz) 138.1, 131.2, 129.0, 127.8, 124.2, 122.1, 120.9, 119.5, 116.3, 115.2, 38.0. HRMS (ESI) Calcd for $C_{19}H_{14}ClF_3N_5O$ [M+H]$^+$: 420.08335, found: 420.08344. Anal. Calcd for C, 54.36; H, 3.12; N, 16.68. Found: C, 54.17; H, 3.49; N, 16.27%.

5-Chloro-*N*-(2-(6-chloro-1*H*-benzimidazol-2-yl)phenyl)-1,3-dimethyl-1*H*-pyrazole-4-carboxamide (T3): White solid, yield 59.6%, mp 231-233 °C; IR (KBr) (ν_{max}/cm^{-1}): 3452, 3205, 1673, 1631, 1590, 1527, 1471, 1432, 1378, 1310, 1274, 1060, 932, 905, 807, 733. ^{1}H NMR (400 MHz, DMSO-d_6) δ: 13.38 (s, 1H), 13.04 (s, 1H), 8.75 (d, J = 8.3 Hz, 1H), 8.20-8.04 (m, 1H), 7.77-7.59 (m, 2H), 7.55 (t, J = 7.8 Hz, 1H), 7.32 (t, J = 7.6 Hz, 2H), 3.87 (s, 3H), 2.45 (s, 3H). ^{13}C NMR (101 MHz, DMSO-d_6) δ:

160.6, 152.3, 148.4, 138.6, 131.3, 128.0, 127.4, 123.6, 121.3, 116.0, 113.4, 36.6, 14.2. HRMS (ESI) Calcd for $C_{19}H_{16}Cl_2N_5O$ $[M+H]^+$: 400.07264, found: 400.07245. Anal. Calcd for C, 57.01; H, 3.78; N, 17.50. Found: C, 57.39; H, 4.22; N, 17.28%.

5-Chloro-*N*-(2-(6-chloro-1*H*-benzimidazol-2-yl)phenyl)-1-methyl-3-(trifluoromethyl)-1*H*-pyrazole-4-carboxamide (T4): White solid, yield 41.5%, mp 225-227 °C; IR (KBr) (ν_{max}/cm^{-1}): 3407, 3226, 1649, 1619, 1539, 1485, 1450, 1399, 1325, 1191, 1155, 1057, 1033, 751. ^{1}H NMR (400 MHz, DMSO-d_6) δ: 13.62 (s, 1H), 13.44 (s, 1H), 8.78 (d, J = 7.8 Hz, 1H), 8.19 (dd, J = 7.9, 1.0 Hz, 1H), 7.71 (s, 1H), 7.65 (d, J = 8.5 Hz, 1H), 7.62–7.55 (m, 1H), 7.37 (dd, J = 11.2, 4.1 Hz, 1H), 7.31 (dd, J = 8.5, 1.3 Hz, 1H), 4.06 (s, 3H). ^{13}C NMR (101 MHz, DMSO-d_6) δ: 157.9, 152.1, 139.2 (q, J= 38.3Hz), 138.1, 131.5, 129.1, 127.9, 124.2, 122.1, 121.0, 119.5, 116.0, 115.0, 38.1. HRMS (ESI) Calcd for $C_{19}H_{13}Cl_2F_3N_5O$ $[M+H]^+$: 454.04438, found: 454.04425. Anal. Calcd for C, 50.24; H, 2.66; N, 15.42. Found: C, 50.65; H, 3.08; N, 15.26%.

5-Chloro-1,3-dimethyl-*N*-(2-(6-methyl-1*H*-benzimidazol-2-yl)phenyl)-1*H*-pyrazole-4-carboxamide (T5): White solid, yield 53.0%, mp 220-222 °C; IR (KBr) (ν_{max}/cm^{-1}): 3280, 2860, 1643, 1613, 1590, 1551, 1524, 1485, 1429, 1363, 1310, 1265, 962. 902, 762, 632, 599. ^{1}H NMR (400 MHz, DMSO-d_6) δ: 13.32 (s, 1H), 13.07 (d, J = 16.9 Hz, 1H), 8.81–8.71 (m, 1H), 8.13 (d, J = 7.9 Hz, 1H), 7.49 (dd, J = 16.1, 8.6 Hz, 2H), 7.40 (d, J = 19.1 Hz, 1H), 7.30 (t, J = 7.6 Hz, 1H), 7.10 (dd, J = 19.3, 8.1 Hz, 1H), 3.86 (s, 3H), 2.46 (t, J = 7.2 Hz, 6H). ^{13}C NMR (101 MHz, DMSO-d_6) δ: 160.6, 150.9, 150.5, 148.1 (d, J = 10.7 Hz), 142.8, 140.62, 138.5, 134.3, 133.3, 132.0, 131.8, 130.7, 127.6 (d, J = 12.8 Hz), 125.3, 124.3, 123.5, 121.2, 118.4 (d, J = 7.4 Hz), 116.4, 113.6, 111.5 (d, J = 14.2 Hz), 36.6, 21.7 (d, J = 17.4 Hz), 14.2. HRMS (ESI) Calcd for $C_{20}H_{19}ClN_5O$ $[M+H]^+$: 380.12726, found: 380.12711. Anal. Calcd for C, 63.24; H, 4.78; N, 18.44. Found: C, 63.68; H, 5.12; N, 18.19%.

5-Chloro-1-methyl-*N*-(2-(6-methyl-1*H*-benzimidazol-2-yl)phenyl)-3-(trifluoromethyl)-1*H*-pyrazole-4-carboxamide (T6): White solid, yield 65.1%, mp 160-162 °C; IR (KBr) (ν_{max}/cm^{-1}): 3416, 3235, 1652, 1613, 1587, 1536, 1488, 1432, 1402, 1316, 1271, 1185, 1149, 1024, 899, 774. ^{1}H NMR (400 MHz, DMSO-d_6) δ: 13.90 (s, 1H), 13.11 (d, J = 17.2 Hz, 1H), 8.81–8.73 (m, 1H), 8.17 (dd, J = 7.9, 1.1 Hz, 1H), 7.61 – 7.31 (m, 4H), 7.11 (dd, J = 22.5, 8.2 Hz, 1H), 4.06 (d, J = 5.9 Hz, 3H), 2.45 (d, J = 11.7 Hz, 3H). ^{13}C NMR (101 MHz, DMSO-d_6) δ: 157.9, 150.7, 150.3, 142.6, 140.4,139.1 (dd, J = 38.1 Hz,5.4 Hz) 138.0 (d, J = 2.2 Hz), 134.1, 133.5, 131.9 (d, J = 5.1 Hz), 131.0 (d, J = 6.1 Hz), 129.1 (d, J = 9.0 Hz), 127.6, 125.4, 124.2 (d, J = 13.9 Hz), 122.1, 120.8 (d, J = 5.9 Hz), 119.5, 118.7 (d, J = 3.2 Hz), 116.4, 115.2, 111.5 (d, J = 11.8 Hz), 38.0 (d, J = 4.8 Hz), 21.8, 21.6. HRMS (ESI) Calcd for $C_{20}H_{16}ClF_3N_5O$ $[M+H]^+$: 434.09900, found: 434.09889. Anal. Calcd for C, 55.37; H, 3.49; N, 16.14. Found: C, 55.86; H, 3.79; N, 15.95%.

***N*-(2-(1*H*-Benzimidazol-2-yl)phenyl)-1,3-dimethyl-1*H*-pyrazole-5-carboxamide (T7)**: White solid, yield 53.5%, mp 245-247 °C; IR (KBr) (ν_{max}/cm^{-1}): 3199, 2961, 1679, 1631, 1613, 1599, 1554, 1435, 1363, 1313, 1277, 1247, 1057, 1018, 962, 771, 730. ^{1}H NMR (400 MHz, DMSO-d_6) δ: 13.90 (s, 1H), 13.29 (s, 1H), 8.80 (d, J = 8.3 Hz, 1H), 8.18 (d, J = 7.4 Hz, 1H), 7.75 (dd, J = 5.6, 2.7 Hz, 1H), 7.63 (dd, J = 5.6, 2.6 Hz, 1H), 7.54 (t, J = 7.6 Hz, 1H), 7.34 (m, 3H), 7.07 (s, 1H), 4.09 (s, 3H), 2.33 (s, 3H). ^{13}C NMR (101 MHz, DMSO-d_6) δ: 158.2, 151.2, 146.3, 142.2, 138.5, 136.6, 133.8, 131.1, 127.6, 124.0, 123.5, 122.9, 120.1, 118.4, 115.8, 112.0, 107.1, 39.1, 13.5. HRMS (ESI) Calcd for $C_{19}H_{18}N_5O$ $[M+H]^+$: 332.15059, found: 332.15085. Anal. Calcd for C, 68.87; H, 5.17; N, 21.13. Found: C, 68.85; H, 5.48; N, 20.73%.

***N*-(2-(1*H*-Benzimidazol-2-yl)phenyl)-3-isobutyl-1-methyl-1*H*-pyrazole-5-carboxamide (T8)**: White solid, yield 51.4%, mp 213-215 °C; IR (KBr) (ν_{max}/cm^{-1}): 3410, 3110, 1634, 1613, 1599, 1551, 1438, 1405, 1316, 1277, 762, 736, 620. ^{1}H NMR (400 MHz, DMSO-d_6) δ: 13.88 (s, 1H), 13.45 (s, 1H), 8.82 (d, J = 7.8 Hz, 1H), 8.22 (t, J = 13.6 Hz, 1H), 7.71–7.61 (m, 2H), 7.54 (dd, J = 11.5, 4.2 Hz, 1H), 7.32 (dd, J = 8.8, 6.5 Hz, 3H), 7.07 (s, 1H), 4.11 (s, 3H), 2.56 (d, J = 7.0 Hz, 2H), 1.99 (m, 1H), 1.01 (s, 3H), 0.99 (s, 3H). ^{13}C NMR (101 MHz, DMSO-d_6) δ: 158.3, 151.3, 150.0, 142.2, 138.5, 136.5, 133.9, 131.1, 127.9, 123.9, 123.6, 122.8, 120.2, 118.1, 115.9, 112.2, 106.8, 39.2, 37.1, 28.9, 22.8. HRMS (ESI) Calcd for $C_{22}H_{24}N_5O$ $[M+H]^+$: 374.19754, found:.374.19775. Anal. Calcd for C, 70.76; H, 6.21; N, 18.75. Found: C, 70.71; H, 6.09; N, 18.95%.

***N*-(2-(6-Chloro-1*H*-benzimidazol-2-yl)phenyl)-1,3-dimethyl-1*H*-pyrazole-5-carboxamide (T9)**: White solid, yield 41.3%, mp 254-256 °C; IR (KBr) (ν_{max}/cm^{-1}): 3410, 2949, 1634, 1616, 1592, 1544, 1446, 1422, 1321, 1288, 937, 777, 634. ^{1}H NMR (400 MHz, DMSO-d_6) δ: 13.57 (d, J = 34.8 Hz, 1H), 13.44 (s, 1H), 8.77 (d, J = 8.3 Hz, 1H), 8.14 (d, J = 7.8 Hz, 1H), 7.79 – 7.47 (m, 3H), 7.32 (dd, J = 16.1, 8.4 Hz, 2H), 6.98 (s, 1H), 4.07 (s, 3H), 2.31 (s, 3H). ^{13}C NMR (101 MHz, DMSO-d_6) δ: 158.0, 146.1, 138.5, 136.4, 131.2, 127.6, 123.3, 120.1, 115.2, 107.0, 39.1, 13.5. HRMS (ESI) Calcd for $C_{19}H_{17}ClN_5O$ $[M+H]^+$: 366.11161, found: 366.11182. Anal. Calcd for C, 62.38; H, 4.41; N, 19.14. Found: C, 62.78; H, 4.84; N, 18.80%.

***N*-(2-(6-Chloro-1*H*-benzimidazol-2-yl)phenyl)-3-isobutyl-1-methyl-1*H*-pyrazole-5-carboxamide (T10)**: White solid, yield 52.4%, mp 194-195 °C; IR (KBr) (ν_{max}/cm^{-1}): 3327, 2946, 1652, 1631, 1616, 1587, 1548, 1447, 1423, 1325, 1304, 1063, 932, 765. ^{1}H NMR (400 MHz, DMSO-d_6) δ: 13.58 (s, 1H), 13.40 (s, 1H), 8.76 (d, J = 8.3 Hz, 1H), 8.17 – 8.05 (m, 1H), 7.65–7.57 (m, 2H), 7.58–7.47 (m, 1H), 7.40–7.18 (m, 2H), 6.95 (s, 1H), 4.08 (s, 3H), 2.53 (d, J = 3.8 Hz, 2H), 1.97 (td, J = 13.3, 6.6 Hz, 1H), 1.01 (s, 3H), 0.99 (s, 3H). ^{13}C NMR (101 MHz, DMSO-d_6) δ: 158.2, 152.6, 149.9, 138.5, 136.4, 131.3, 127.7, 127.5, 123.4, 120.2, 115.5, 106.6, 39.1, 37.1, 28.8, 22.8. HRMS (ESI) Calcd for $C_{22}H_{23}ClN_5O$ $[M+H]^+$: 408.15856, found: 408.15866. Anal. Calcd for C, 64.78; H, 5.44; N, 17.17. Found: C, 64.98; H, 5.82; N, 16.83%.

1,3-Dimethyl-*N*-(2-(6-methyl-1*H*-benzimidazol-2-yl)phenyl)-1*H*-pyrazole-5-carboxamide (T11): White solid, yield 66.1%, mp 256-258 °C; IR (KBr) (ν_{max}/cm^{-1}): 3309, 2914, 1685, 1640, 1616, 1593, 1542, 1485, 1435, 1319, 1280, 1021, 751. ^{1}H NMR (400 MHz, DMSO-d_6) δ: 13.90 (s, 1H), 13.13 (d, J = 13.6 Hz, 1H), 8.79 (d, J = 8.4 Hz, 1H), 8.15 (d, J = 7.9 Hz, 1H), 7.64–7.37 (m, 3H), 7.30 (t, J = 7.5 Hz, 1H), 7.15 (t, J = 8.2 Hz, 1H), 7.05 (s, 1H), 4.09 (s, 3H), 2.48 (s, 3H), 2.32 (d, J = 3.8 Hz, 3H). ^{13}C NMR (101 MHz, DMSO-d_6) δ: 158.2, 151.0, 150.7, 146.2, 142.6, 140.4, 138.4 (d, J = 4.8 Hz), 136.6, 134.1, 133.4, 131.9 (d, J = 5.4 Hz),

View Article Online
DOI: 10.1039/C8NJ05138A

130.9 (d, *J* = 5.4 Hz), 127.5, 125.4, 124.4, 123.4, 120.1, 118.0 (d, *J* = 12.4 Hz), 115.9, 111.6 (d, *J* = 15.5 Hz), 107.1, 21.8 (d, *J* = 10.0 Hz), 13.5. HRMS (ESI) Calcd for $C_{20}H_{20}N_5O$ $[M+H]^+$: 346.16624, found: 346.16632. Anal. Calcd for C, 69.55; H, 5.54; N, 20.28. Found: C, 69.24; H, 5.56; N, 20.03%.

3-Isobutyl-1-methyl-*N*-(2-(6-methyl-1*H*-benzimidazol-2-yl)phenyl)-1*H*-pyrazole-5-carboxamide (T12): White solid, yield 51.7%, mp 180-182 °C; IR (KBr) (ν_{max}/cm^{-1}): 3324, 2952, 1640, 1619, 1589, 1550, 1491, 1431, 1407, 1306, 1268, 1169, 1062, 1015, 967, 595. ^{1}H NMR (400 MHz, DMSO-d_6) δ: 13.91 (d, *J* = 34.3 Hz, 1H), 13.15 (d, *J* = 17.1 Hz, 1H), 8.80 (dd, *J* = 8.2, 3.5 Hz, 1H), 8.15 (d, *J* = 8.0 Hz, 1H), 7.59–7.48 (m, 2H), 7.43 (d, *J* = 23.1 Hz, 1H), 7.31 (t, *J* = 7.6 Hz, 1H), 7.16 (t, *J* = 8.0 Hz, 1H), 7.06 (d, *J* = 10.7 Hz, 1H), 4.10 (s, 3H), 2.58–2.53 (m, 2H), 2.47 (d, *J* = 9.7 Hz, 3H), 2.08–1.92 (m, 1H), 1.01 (dd, *J* = 10.9, 6.6 Hz, 6H). ^{13}C NMR (101 MHz, DMSO-d_6) δ: 158.3 (d, *J* = 4.2 Hz), 151.1, 150.7, 149.9 (d, *J* = 6.0 Hz), 142.5, 140.4, 138.4 (d, *J* = 8.6 Hz), 136.5 (d, *J* = 7.7 Hz), 134.1, 133.5, 131.8 (d, *J* = 11.4 Hz), 130.9 (d, *J* = 5.9 Hz), 127.5, 125.3, 124.4, 123.5, 120.1, 117.9, 117.7, 116.0 (d, *J* = 3.3 Hz), 111.6 (d, *J* = 15.1 Hz), 106.7 (d, *J* = 9.7 Hz), 37.1, 28.9 (d, *J* = 5.4 Hz), 22.8 (d, *J* = 2.7 Hz), 21.7 (d, *J* = 16.3 Hz). HRMS (ESI) Calcd for $C_{23}H_{26}N_5O$ $[M+H]^+$: 388.21319, found: 388.21304. Anal. Calcd for C, 71.29; H, 6.50; N, 18.07. Found: C, 71.29; H, 6.53; N, 17.85%.

***N*-(2-(1*H*-Benzimidazol-2-yl)phenyl)niacinamide (T13)**: White solid, yield 69.6%, mp 235-237 °C; IR (KBr) (ν_{max}/cm^{-1}): 3410, 3288, 1634, 1619, 1599, 1545, 1485, 1435, 1402, 1319, 1197, 965. ^{1}H NMR (400 MHz, DMSO-d_6) δ: 14.23 (s, 1H), 13.34 (s, 1H), 9.41 (d, *J* = 1.6 Hz, 1H), 8.96–8.85 (m, 2H), 8.58 (d, *J* = 8.0 Hz, 1H), 8.22 (d, *J* = 7.9 Hz, 1H), 7.77 (dd, *J* = 7.5, 5.1 Hz, 2H), 7.64 (d, *J* = 7.0 Hz, 1H), 7.58 (t, *J* = 7.9 Hz, 1H), 7.39–7.29 (m, 3H). ^{13}C NMR (101 MHz, DMSO-d_6) δ: 163.8, 152.9, 151.3, 149.1, 142.1, 138.6, 135.3, 133.8, 131.2, 130.8, 127.6, 124.3, 124.0, 123.8, 122.9, 120.4, 118.5, 116.1, 112.0. HRMS (ESI) Calcd for $C_{19}H_{15}N_4O$ $[M+H]^+$: 315.12404, found: 315.12411. Anal. Calcd for C, 72.60; H, 4.49; N, 17.82. Found: C, 72.29; H, 4.62; N, 17.48%.

***N*-(2-(1*H*-Benzimidazol-2-yl)phenyl)-2-chloroniacinamide (T14)**: White solid, yield 80.5%, mp 203-205 °C; IR (KBr) (ν_{max}/cm^{-1}): 3229, 2991, 1700, 1628, 1599, 1548, 1485, 1435, 1399, 1319, 1277, 1244, 1137, 1072, 745. ^{1}H NMR (400 MHz, DMSO-d_6) δ: 13.87 (s, 1H), 13.28 (s, 1H), 8.82 (d, *J* = 8.3 Hz, 1H), 8.70–8.63 (m, 1H), 8.38–8.30 (m, 1H), 8.21 (d, *J* = 7.8 Hz, 1H), 7.71 (dd, *J* = 7.5, 4.9 Hz, 1H), 7.66–7.56 (m, 2H), 7.46–7.35 (m, 2H), 7.30 (t, *J* = 7.5 Hz, 1H), 7.23 (t, *J* = 7.5 Hz, 1H). ^{13}C NMR (101 MHz, DMSO-d_6) δ: 163.8, 151.7, 151.0, 147.2, 142.1, 139.0, 138.2, 133.8, 133.0, 131.3, 127.8, 124.3, 124.0, 123.8, 122.8, 120.6, 118.7, 116.5, 112.0. HRMS (ESI) Calcd for $C_{19}H_{14}ClN_4O$ $[M+H]^+$: 349.08507, found: 349.08511. Anal. Calcd for C, 65.43; H, 3.76; N, 16.06. Found: C, 65.82; H, 4.14; N, 15.77%.

***N*-(2-(1*H*-Benzimidazol-2-yl)phenyl)-2-mercaptoniacinamide (T15)**: Yellow solid, yield 42.0%, mp 207-209 °C; IR (KBr) (ν_{max}/cm^{-1}): 3416, 2955, 1661, 1575, 1527, 1432, 1322, 1298, 1241, 1137, 1075, 757. ^{1}H NMR (400 MHz, DMSO-d_6) δ: 13.89 (s, 1H), 13.33 (s, 1H), 13.12 (s, 1H), 8.70 (d, *J* = 8.1 Hz, 1H), 8.08 (d, *J* = 7.6 Hz, 1H), 7.99 (d, *J* = 6.8 Hz, 1H), 7.88 (d, *J* = 5.4 Hz, 1H), 7.62–7.45 (m, 3H), 7.31 (dd, *J* = 14.9, 7.4 Hz, 1H), 7.23 (d, *J* = 8.7 Hz, 2H), 6.94 (t, *J* = 6.6 Hz, 1H). ^{13}C NMR (101 MHz, DMSO-d_6) δ: 174.8, 165.0, 150.7, 140.7, 139.0, 138.8, 138.2, 130.9, 128.5, 123.9, 121.5, 118.0, 113.1. HRMS (ESI) Calcd for $C_{19}H_{15}N_4OS$ $[M+H]^+$: 347.09611, found: 347.09616. Anal. Calcd for C, 65.88; H, 4.07; N, 16.17. Found: C, 65.39; H, 3.89; N, 15.92%.

***N*-(2-(6-Chloro-1*H*-benzimidazol-2-yl)phenyl)nicotinamide (T16)**: White solid, yield 65.3%, mp 300-302 °C; IR (KBr) (ν_{max}/cm^{-1}): 3324, 2896, 1661, 1634, 1504, 1548, 1480, 1441, 1390, 1325, 1262, 1060, 965, 768, 727, 599. ^{1}H NMR (400 MHz, DMSO-d_6) δ: 13.88 (s, 1H), 13.46 (s, 1H), 9.34 (d, *J* = 1.7 Hz, 1H), 8.87 (dd, *J* = 4.6, 3.6 Hz, 2H), 8.51 (d, *J* = 8.0 Hz, 1H), 8.15 (d, *J* = 7.9 Hz, 1H), 7.75 (dt, *J* = 14.5, 7.3 Hz, 1H), 7.66 (s, 2H), 7.57 (t, *J* = 7.8 Hz, 1H), 7.32 (t, *J* = 7.2 Hz, 2H). ^{13}C NMR (101 MHz, DMSO-d_6) δ: 163.6, 152.8, 152.5, 148.9, 138.6, 135.3, 131.5, 130.6, 127.7, 124.4, 123.7, 120.4, 115.6. HRMS (ESI) Calcd for $C_{19}H_{14}ClN_4O$ $[M+H]^+$: 349.08507, found: 349.08527. Anal. Calcd for C, 65.43; H, 3.76; N, 16.06. Found: C, 65.75; H, 4.01; N, 16.22%.

2-Chloro-*N*-(2-(6-chloro-1*H*-benzimidazol-2-yl)phenyl)niacinamide (T17): White solid, yield 49.1%, mp 228-230 °C; IR (KBr) (ν_{max}/cm^{-1}): 3419, 2993, 1699, 1640, 1616, 1538 , 1479, 1431, 1348, 1309, 1146, 1056, 747. ^{1}H NMR (400 MHz, DMSO-d_6) δ: 13.53 (d, *J* = 25.1 H, 1H), 13.43 (s, s, 1H), 8.78 (d, *J* = 8.3 Hz, 1H), 8.65 (d, *J* = 4.6 Hz, 1H), 8.31 (d, *J* = 7.6 Hz, 1H), 8.17 (d, *J* = 7.9 Hz, 1H), 7.71 (td, *J* = 8.3, 5.0 Hz, 1H), 7.61 (t, *J* = 8.0 Hz, 2H), 7.50 – 7.35 (m, 2H), 7.28 (dd, *J* = 29.8, 8.5 Hz, 1H). ^{13}C NMR (101 MHz, DMSO-d_6) δ: 163.8, 151.7, 147.2, 138.9, 138.2, 132.8, 131.6, 128.0, 124.3, 123.9, 120.7, 118.0, 116.2. HRMS (ESI) Calcd for $C_{19}H_{13}Cl_2N_4O$ $[M+H]^+$: 383.04609, found: 383.04617. Anal. Calcd for C, 59.55; H, 3.16; N, 14.62. Found: C, 59.75; H, 3.50; N, 14.39%.

***N*-(2-(6-Chloro-1*H*-benzimidazol-2-yl)phenyl)-2-mercaptoniacinamide (T18)**: Yellow solid, yield 43.8%, mp 215-217 °C; IR (KBr) (ν_{max}/cm^{-1}): 3416, 3309, 2905, 1637, 1587, 1539, 1485, 1426, 1396, 1331, 1247, 1155, 1057, 742. ^{1}H NMR (400 MHz, DMSO-d_6) δ: 13.93 (s, 1H), 13.26 (s, 1H), 13.18 (s, 1H), 8.67 (d, *J* = 8.2 Hz, 1H), 8.11 – 7.99 (m, 2H), 7.90 (d, *J* = 5.3 Hz, 1H), 7.56 (d, *J* = 9.4 Hz, 3H), 7.32 (dd, *J* = 15.5, 8.0 Hz, 1H), 7.26 (s, 1H), 6.96 (t, *J* = 6.7 Hz, 1H). ^{13}C NMR (101 MHz, DMSO-d_6) δ: 174.6, 164.8, 141.0, 139.7, 138.1, 138.0, 131.2, 128.9, 124.1, 121.9, 118.3, 113.2. HRMS (ESI) Calcd for $C_{19}H_{14}ClN_4OS$ $[M+H]^+$: 381.05714, found: 381.05685. Anal. Calcd for C, 59.92; H, 3.44; N, 14.71. Found: C, 59.97; H, 3.92; N, 14.28%.

***N*-(2-(6-Methyl-1*H*-benzimidazol-2-yl)phenyl)niacinamide (T19)**: White solid, yield 72.4%, mp 259-260 °C; IR (KBr) (ν_{max}/cm^{-1}): 3324, 2854, 1661, 1634, 1616, 1593, 1551, 1485, 1441, 1396, 1322, 1024, 765. ^{1}H NMR (400 MHz, DMSO-d_6) δ: 14.24 (s, 1H), 13.17 (d, *J* = 16.8 Hz, 1H), 9.46–9.35 (m, 1H), 8.98–8.80 (m, 2H), 8.56 (d, *J* = 8.0 Hz, 1H), 8.19 (d, *J* = 7.9 Hz, 1H), 7.76 (dt, *J* = 8.0, 5.1 Hz, 1H), 7.65–7.38 (m, 3H), 7.33 (t, *J* = 7.3 Hz, 1H), 7.15 (t, *J* = 9.3 Hz, 1H), 2.48 (s, 3H). ^{13}C NMR (101 MHz, DMSO-d_6) δ: 163.7, 152.8, 151.1, 150.7, 149.1 (d, *J*= 8.8 Hz), 142.5, 140.3, 138.5 (d, *J*= 4.4 Hz), 135.4 (d, *J*= 7.3 Hz), 134.0, 133.5, 131.9, 131.8, 130.9 (d, *J*= 6.9 Hz), 130.8, 127.4, 125.5, 124.4, 124.3 (d, *J*= 3.9 Hz), 123.7, 120.3, 118.1 (d, *J*= 8.7

View Article Online DOI: 10.1039/C9NJ05501J

Hz), 116.2, 111.6, 111.5, 21.8, 21.7. HRMS (ESI) Calcd for $C_{20}H_{17}N_4O$ $[M+H]^+$: 329.13969, found: 329.13992. Anal. Calcd for C, 73.15; H, 4.91; N, 17.06. Found: C, 72.84; H, 4.92; N, 16.89%.

2-Chloro-*N*-(2-(6-methyl-1*H*-benzimidazol-2-yl)phenyl)niacinamide (T20): White solid, yield 70.3%, mp 150-152 °C; IR (KBr) (ν_{max}/cm^{-1}): 3249, 2919, 1699, 1635, 1613, 1600, 1549, 1484, 1431, 1405, 1388, 1314, 1269, 1148, 1064, 799, 753. ^{1}H NMR (400 MHz, DMSO-d_6) δ: 13.90 (s, 1H), 13.14 (d, J = 17.8 Hz, 1H), 8.82 (d, J = 8.1 Hz, 1H), 8.66 (d, J = 3.0 Hz, 1H), 8.33 (dd, J = 7.6, 1.7 Hz, 1H), 8.18 (d, J = 7.9 Hz, 1H), 7.71 (dd, J = 12.1, 6.1 Hz, 1H), 7.58 (t, J = 7.8 Hz, 1H), 7.50–7.34 (m, 2H), 7.32–7.18 (m, 1H), 7.08 (dd, J = 30.7, 8.1 Hz, 1H), 2.42 (d, J = 19.7 Hz, 3H). ^{13}C NMR (101 MHz, DMSO-d_6) δ: 163.8, 151.7, 147.2, 138.9, 138.1, 133.0, 131.1, 127.6, 124.2, 123.9, 120.5, 118.3, 116.5, 111.6, 21.7 (d, J= 21.2Hz). HRMS (ESI) Calcd for $C_{20}H_{16}ClN_4O$ $[M+H]^+$: 363.10072, found: 363.10059. Anal. Calcd for C, 66.21; H, 4.17; N, 15.44. Found: C, 66.62; H, 4.42; N, 15.29%.

Crystallographic study

The single crystal of **T1** was obtained from the mixed liquor of chloroform and ethyl acetate (V/V = 2:3). The single crystal X-ray diffraction data were collected on an Agilent SuperNova (Dual, Cu at zero, AtlasS2) diffractometer at 100.00(10) K using Mo Kα radiation (λ = 0.71073 Å) by the ω scan mode. The program CrysAlisPro was used for integration of the diffraction profiles.[29] The structure was solved by direct methods using the SHELXS program of the SHELXTL package and refined by full-matrix least-squares methods with SHELXL.[30] All non-hydrogen atoms of the compound **T1** were refined with anisotropic thermal parameters. All hydrogen atoms were observed and placed at their calculated positions with a fixed value of their isotropic displacement parameters.

In vitro antifungal bioassay

The antifungal activities were evaluated against four pathogenic fungi (*B. cinerea, R. solani and F. graminearum, A. solani*) *in vitro* with a mycelia growth test on potato dextrose agar medium (PDA).[2,31] The mother liquor (22.5 mg/mL) was prepared by dissolving the compound (18 mg) in DMSO (0.8 mL). 0.2 ML of mother liquor was mixed with sterile molten PDA (45 mL) to obtain the PDA with the test compound at final concentration of 100 ug/mL. The portions of PDA with different compounds were poured into three Petri dishes (90 mm in diameter) on average (15 mL/dish), on which 5-mm mycelial disks of the four fungi were placed at the center. The disks were obtained from a pure PDA culture plate by punching at the edge of the actively growing mycelia colony. Each treatment condition was produced in three replicates. The commercial fungicide hymexazol was served as the positive control.

After a certain incubation period (1.5 d for *R. solani*, 2.5 d for *B. cinerea*, 3.5 d for *F. graminearum*, and 5 d for *A. solani*, according to their respective mycelia growth rates) at 25±1°C in a dark environment, the diameters of mycelial colony were measured, and the data were statistically analyzed. The inhibitory percentages of the title compounds *in vitro* against these fungi were calculated as I (%)=[(C−T)/ (C−0.5)]×100, where C represents the diameter of colony on untreated PDA, T represents the diameter of colony on treated PDA, and I represents the inhibition rate. Furthermore, the fungicidal activities of these compounds against *B. cinerea* were further assessed. As per the preliminary test record, these compounds were dissolved in DMSO and diluted with the medium to obtain different final concentration grades. The colony diameters were measured, and the inhibition percentages relative to the blank control were calculated. The EC_{50} values were finally obtained via linear-regression analysis.

3D-QSAR analysis

The molecular modeling and CoMFA analysis were performed using SYBYL 2.0 software. The 3D structures of all molecules were built using the Sketch Molecule function in SYBYL. The initial structural optimization was conducted using the Gasteiger−Huckel charge, Tripos force field, and Powell conjugate gradient algorithm with a convergence criterion of 0.005 kcal/mol Å.[32]

The 3D-QSAR modeling was derived using the partial least square (PLS) analysis. The interaction energies between a probe atom and all compounds were computed at surrounding points by using a volume dependent lattice with a 2.0 grid spacing (default in SYBYL).[33] The CoMFA descriptors were used as independent variables, and the experimental pEC_{50} values were presented as the dependent variables. The performance of the models was evaluated by leave-one-out cross-validation, and the optimal number of components (ONC) was determined with the highest cross-validated q^2.[34,35] The non-cross-validated correlation coefficient r^2, standard error of estimate (SEE), and F were subsequently calculated according to the definitions in the SYBYL 2.0 package. The contour maps and standard deviations of CoMFA were generated by using PLS coefficients.

Conflicts of interest

There are no conflicts to declare.

Acknowledgements

This work was supported by the National Nature Science Foundation of China (No. 31772209) and the Fundamental Research Funds for the Central Universities of China (No. KYTZ201604 and KJSY201607).

Notes and references

1 M. C. Fisher, D. A. Henk, C. J. Briggs, J. S. Brownstein, L. C. Madoff, S. L. McCraw and S. J. Gurr, *Nature*, 2012, **484**, 186.
2 J. J. Wang, W. J. Si, M. Chen, A. M. Lu, W. H. Zhang and C. L. Yang, *J. Pestici. Sci.*, 2017, **42**, 84−92.
3 J. Cooper and H. Dobson, *Crop Prot.*, 2007, **26**, 1337-1348.
4 B. Williamson, B. Tudzynski, P. Tudzynski and J. A. van Kan, *Mol. Plant Pathol.*, 2007, **8**, 561−580.
5 B. Sneh, S. Jabaji-Hare, S. Neate and G. Dijst, *Rhizoctonia species: taxonomy, molecular biology, ecology, pathology*

and disease control, Springer Science & Business Media, 2013.
6 R. S. Goswami and H. C. Kistler, *Mol. Plant Pathol.*, 2004, **5**, 515–525.
7 W. Fry, *Mol. Plant Pathol.*, 2008, **9**, 385–402.
8 R. Dean, J. A. Van Kan, Z. A. Pretorius, K. E. Hammond - Kosack, A. Di Pietro, P. D. Spanu, J. J. Rudd, M. Dickman, R. Kahmann and J. Ellis, *Mol. Plant Pathol.*, 2012, **13**, 414–430.
9 J. A. Davidson, S. Pande, T. W. Bretag, K. D. Lindbeck and G. Krishna-Kishore, *Botrytis: biology, pathology and control*, Springer, 2007, pp. 295–318.
10 P. Leroux, R. Fritz, D. Debieu, C. Albertini, C. Lanen, J. Bach, M. Gredt and F. Chapeland, *Pest Manag. Sci.*, 2002, **58**, 876–888.
11 W. Aktar, D. Sengupta and A. Chowdhury, *Interdiscipl. Toxicol.*, 2009, **2**, 1–12.
12 N. Singh, A. Pandurangan, K. Rana, P. Anand, A. Ahamad and A. K. Tiwari, *Int. Curr. Pharm. J.,* 2012, **1**, 119–127.
13 H. M. Refaat, *Eur. J. Med. Chem.*, 2010, **45**, 2949–2956.
14 P. A. Thakurdesai, S. G. Wadodkar and C. T. Chopade, *Pharmaco.*, 2007, **1**, 314–329.
15 K. Starčević, M. Kralj, K. Ester, I. Sabol, M. Grce, K. Pavelić and G. Karminski-Zamola, *Bioorg. Med. Chem.*, 2007, **15**, 4419–4426.
16 R. V. Shingalapur, K. M. Hosamani and R. S. Keri, *Eur. J. Med. Chem.*, 2009, **44**, 4244–4248.
17 A. Khalafi-Nezhad, M. S. Rad, H. Mohabatkar, Z. Asrari and B. Hemmateenejad, *Bioorg. Med. Chem.*, 2005, **13**, 1931–1938.
18 Y. B. Bai, A. L. Zhang, J. J. Tang and J. M. Gao, *J. Agric. Food. Chem.*, 2013, **61**, 2789–2795.
19 K. Fujii and T. Tallaka, *JP Patent* 7285942, 1995.
20 I. Okada, S. Okui and T. Nakajima, *JP Patent* 91206709, 1991.
21 J. Wu, Q. Shi, Z. Chen, M. He, L. Jin and D. Hu, *Molecules*, 2012, **17**, 5139–5150.
22 H. Dai, Y.-Q. Li, D. Du, X. Qin, X. Zhang, H.-B. Yu and J.-X. Fang, *J. Agric. Food. Chem.*, 2008, **56**, 10805–10810.
23 D. Huang, M. Huang, A. Liu, X. Liu, W. Liu, X. Chen, H. Xue, J. Sun, D. Yin and X. Wang, *J. Heterocycl. Chem.*, 2017, **54**, 1121–1128.
24 P. V. Patel, N. Joshi and D. P. Panchal, *Heterocycl. Lett.*, 2012, **2**, 467–478.
25 G. Coban, S. Zencir, I. Zupkó, B. Réthy, H. S. Gunes and Z. Topcu, *Eur. J. Med. Chem.*, 2009, **44**, 2280–2285.
26 L. Keurulainen, O. Salin, A. Siiskonen, J. M. Kern, J. Alvesalo, P. Kiuru, M. Maass, J. Yli-Kauhaluoma and P. Vuorela, *J. Med. Chem.*, 2010, **53**, 7664–7674.
27 A. Golbraikh and A. Tropsha, *J. Mol. Graph. Model.*, 2002, **20**, 269–276.
28 X. Wang, J. Yan, M. Wang, M. Liu, J. Zhang, L. Chen and W. Xue, *Mol. Divers.*, 2018, 1–12.
29 Agilent C.P. CrysAlis PRO. Agilent Technologies, Yarnton, Oxfordshire, England 2013.
30 Sheldrick, G.M. *Acta Crystallogr. A.*, 2008, **64**, 112–122.
31 M. Zhang, Z.-C. Dai, S.-S. Qian, J.-Y. Liu, Y. Xiao, A.-M. Lu, H.-L. Zhu, J.-X. Wang and Y.-H. Ye, *J. Agric. Food. Chem.*, 2014, **62**, 9637–9643.
32 X. Y. Huang, Z. J. Shan, H. L. Zhai, L. N. Li and X. Y. Zhang, *J. Chem. Inf. Model.*, 2011, **51**, 1999-2006.
33 E. A. Amin and W. J. Welsh, *J. Chem. Inf. Model.*, 2006, **46**, 1775–1783.
34 G. Cruciani, M. Baroni, S. Clementi, G. Costantino, D. Riganelli and B. Skagerberg, *J. Chemometr.*, 1992, **6**, 335–346.
35 F. Xu, Y. Wang, D. Luo, G. Yu, S. Guo, H. Fu, Y. Zhao and J. Wu, *RSC Adv.*, 2018, **8**, 6306–6314.

View Article Online
DOI: 10.1039/C8NJ05150J

Design, synthesis, antifungal activity and 3D-QSAR study of novel pyrazole carboxamide and niacinamide derivatives containing benzimidazole moiety

Wei-Jie Si, Xiao-bin Wang, Min Chen, Meng-Qi Wang, Ai-Min Lu and Chun-Long Yang

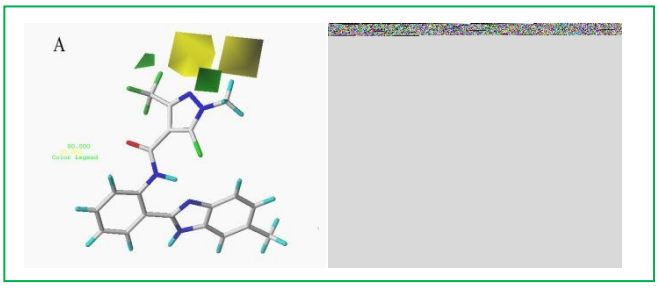

The synthesized pyrazole carboxamide and niacinamide derivatives containing a benzimidazole moiety showed effectively inhibition against the fungus *B. cinerea*. The 3D-QSAR model was built and revealed fine predictive ability.